INTERNATIONAL JOURNAL OF AUTOMOTIVE AND MECHANICAL ENGINEERING
ISSN: 2229-8649 e-ISSN: 2180-1606
VOLUME 23, ISSUE 2, 2026, 13528 - 13542
DOI: https://doi.org/10.15282/ijame.23.2.2026.5.1024

RESEARCH ARTICLE

Optimized drying of Thai Jinda chili peppers using a direct-heating air tray system: Enhancing efficiency and product quality

Ni-Asri Cheputeh[1] and Natthaporn Kaewchoothong[2]*

[1]Department of Mechanical and Mechatronics Engineering, Faculty of Engineering, Prince of Songkla University, Hat Yai, Songkhla 90112, Thailand
[2]Research Center for Energy and Environmental Sustainability, Prince of Songkla University, Hat Yai, Songkhla 90110, Thailand

Abstract - Since foods have naturally high amounts of water content, they are prone to microorganism growth and chemical decomposition. This research aims to explore the drying process of Thai Jinda chilies pepper (TJCPs) in the form of hot-air convection drying by means of a direct-heating perforated air tray (1.5×0.6×1.0 m^3). The effects of different temperatures (55, 60, 65, 70, and 75 °C) and Reynolds numbers (20000, 30000, 40000, and 50000) were studied. As the results indicated, the increase in drying temperature and Reynolds number significantly accelerated the drying process of the samples. The optimal drying conditions were achieved by performing tests at 75 °C and Re = 50000; this led to the minimum drying time of about 6-7 hours without deteriorating the physical properties of TJCPs. The effective moisture diffusivity increased between 0.374×10^{-10} and 5.176×10^{-10} m^2/s while the activation energy decreased in correlation with the airflow intensity. This can be explained by the enhancement of heat and mass transfer due to an intense airflow circulation, thinning of the thermal boundary layer, and efficient convective transport inside the drying chamber. It is concluded that the perforated air tray method is an effective way to enhance thermo-fluid drying of TJCPs.

Article History
Received : 3 October 2025
Revised : 6 May 2026
Accepted : 19 May 2026
Published : 30 June 2026

Keywords
Thai Jinda chili pepper
Quality characteristic
Moisture diffusivity
Activation energy
Direct-heating air trays
Drying kinetic

1. Introduction

Chilies (*Capsicum annuum* L.) are widely consumed in Thailand, with at least 79 distinct varieties such as Prik Yuak, Thai Prik Num, Thai Prik Chi Fah, Jinda chili, and Bird's Eye chili (Figure 1). Among these, Thai Jinda chili peppers (TJCPs, Prik Sod) are commonly used, particularly in soups, due to its moderate spiciness and elongated shape. Color and taste are the main quality attributes that determine its market value. However, after harvest, fresh chilies contain a high moisture content, approximately 75–80% on a wet basis (equivalent to 300–400% on a dry basis), making them highly perishable with a shelf life of only two to three days.

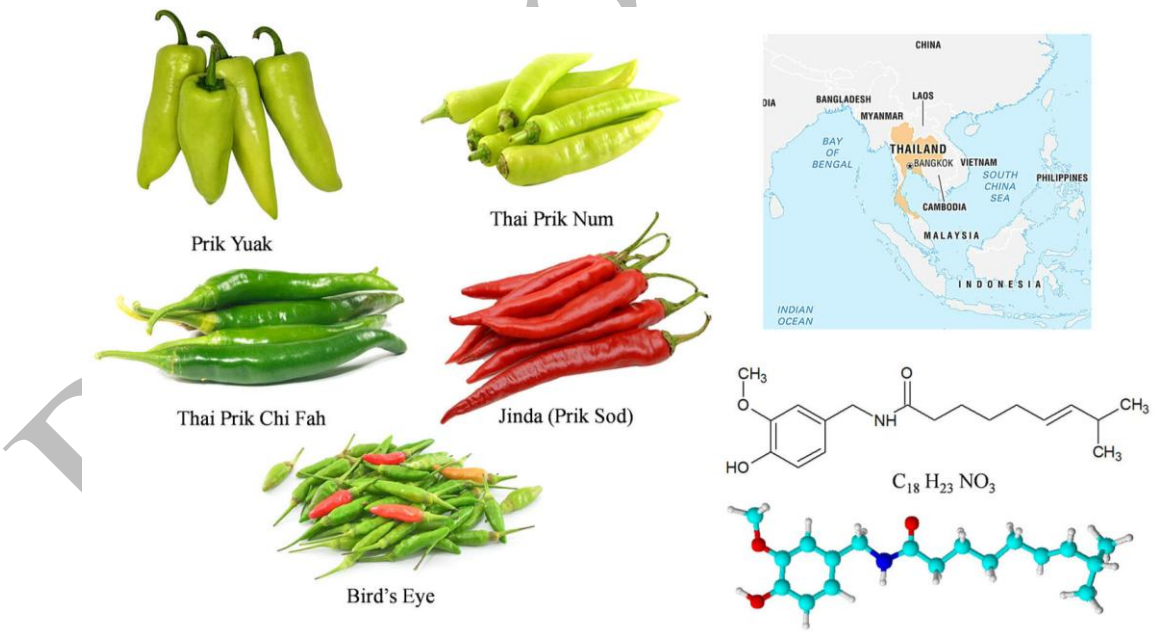

Figure 1. Example of Thai chili peppers

Fruit and vegetable drying remains a popular way of preserving food by removing enough water to prevent both bacterial development and deterioration through chemical means [1, 2]. Vegetable drying should aim at removing enough water, ensuring the desired quality of the product, and keeping operating costs low [3]. Sun drying, which is commonly practiced in Thailand's countryside, is susceptible to environmental changes, insect infestations, and weather conditions [4-6], causing losses of about 30 to 40 percent after harvest [7-9]. In sun-drying, the crops are subjected to direct exposure

*CORRESPONDING AUTHOR | Natthaporn Kaewchoothong | ✉ natthaporn.k@psu.ac.th

to sunlight, which results in non-uniform dehydration and causes deterioration of the qualities that affect the appearance of the product in terms of color, taste, and texture [10-12]. In addition, since the process lacks scientific control of temperatures and humidity, there is vitamin loss, among other nutritional losses [13]. With that, modern drying methods have emerged, focusing on scientific control for effective drying processes [14, 15].

The HACD technique has been broadly applied in the drying of red chilies due to several factors, including simplicity and efficacy in drying while ensuring the production of quality dried products [16]. In the HACD process, the use of air heating enhances dehydration by facilitating the removal of water content while maintaining their color and taste without causing microbial spoilage [17]. Several researchers have found that temperature level greatly affects drying since the drying rate is increased with an increase in drying temperature, but it also affects color and nutrition retention [18, 19]. Different from the traditional hot-air convective dryers that use air circulation for most of their heat transfer process, the current system utilizes a direct-heating mechanism with perforated trays for the enhancement of airflow contact with the surface of the product. This design leads to better forced convection heat transfer with fewer stagnant air zones within the chamber.

Besides the thermal energy supply, the operation of the hot air convection drying process is controlled by various factors such as airflow hydrodynamics, turbulence, heat transfer, and internal moisture diffusion. Airflow hydrodynamics and heat transfer effects play a vital role in determining the temperature distribution, drying rate, and mass diffusion of moisture inside the drying chamber. An increase in airflow speed increases the Reynolds number, resulting in increased forced convection flow that tends to decrease the thermal and mass boundary layer thicknesses around the food product and increase mass and heat transfer rates. This means that the hot air convection dryer should be viewed not only as a processing unit but also as a thermo-fluid system. Recent advancements in HACD strategies have demonstrated superior performance across diverse agricultural commodities. For instance, controlled hot-air drying has been shown to enhance both drying kinetics and bioactive retention in products such as hog plum [20], green banana flour [21], ginger [22], and Radix Ophiopogonis [23]. This improvement in quality extends to the sensory and nutritional attributes of crops like sweet potato chips, as observed by Gonçalves et al. [24]. However, while past researchers have demonstrated that raising the drying temperature and increasing the air velocity improve drying performance, existing research has paid little attention to the thermo-fluid characteristics of drying processes, especially the interplay among fluid dynamics of the air, forced convection with respect to Reynolds numbers, and moisture migration inside direct-heating tray dryers.

Furthermore, the thermo-fluid characteristics of the perforated direct-heating air tray drying system for Thai Jinda chili pepper (TJCP) have yet to be fully explored. The impact of airflow distribution, turbulence-induced convection, and Reynolds number-based drying process on diffusivity, activation energy, and drying uniformity for this chili is yet to be understood. From the standpoint of mechanical engineering, enhancing the process of drying is linked to optimizing the airflow circulation, heat management, and convection processes in the drying chamber. Factors like the temperature of the drying process, air velocity, Reynolds number, and the design of the chamber will impact the convection heat transfer coefficient and moisture diffusion.

Since drying performance and quality retention depend on the nature of the chili cultivar, it becomes imperative to customize the drying conditions based on these unique features. The selection of temperature and air flow rate for drying needs to take into account the rate of moisture migration and stability of chemicals present. In addition, the water evaporation rate during drying affects the rehydratability and market quality of the produce. For this reason, this research is aimed at conducting an experimental study on the thermo-fluid and drying behavior of Thai Jinda chili peppers (TJCPs) through a direct-heating hot air convection dryer under different values of Reynolds number and drying temperature. Particular emphasis is placed on the effect of flow hydrodynamics, improvement of convective heat transfer, diffusion of moisture, activation energy, and drying homogeneity. In addition, the study also aims to analyze the thermo-fluid performance of the perforated tray dryer system in comparison with previous studies on hot air drying.

2. Materials and Methods

2.1 Materials

Fresh Thai Jinda chili peppers (TJCPs) (*Capsicum annuum* L.) were purchased from a local market in Hat Yai, Songkhla, Thailand. Samples were carefully selected based on high moisture content, typically 300–400% on a dry basis (70–90% on a wet basis) [25-27]. Figure 2 presents representative samples of the selected TJCPs.

Figure 2. Example of the selected TJCPs

The geometric properties of the TJCPs, as shown in Figure 3, were characterized using roundness (r), sphericity (s), and cylindricity (c). These three parameters can be calculated using Equations (1) to (3) [25, 27]:

$$r = \frac{A_p}{A_c} \tag{1}$$

$$s = \frac{d_i}{d_c} \tag{2}$$

$$c = \sqrt[3]{\left(\frac{D_i^2 L_i}{D_c^2 L_c}\right)} \tag{3}$$

where A_p and A_c represent the projected area and the smallest circumscribing circle area, respectively; d_i and d_c denote the largest inscribing and smallest circumscribing sphere diameters; D_i, L_i, D_c, and L_c are the diameters and lengths of the largest inscribing and smallest circumscribing cylinders.

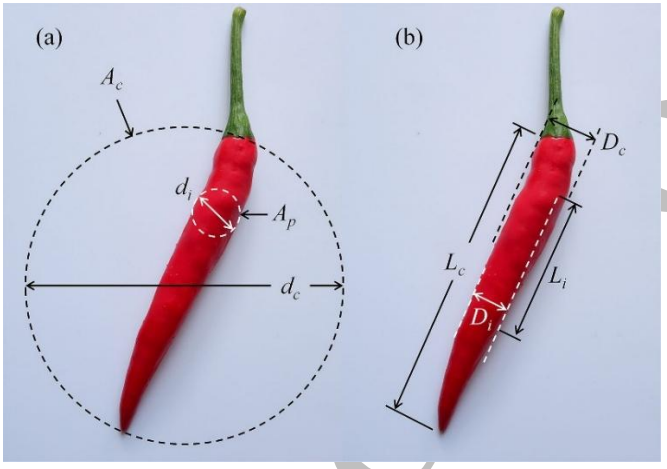

Figure 3. Descriptions of (a) roundness and sphericity and (b) cylindricity of the TJCP

Before drying, TJCPs of uniform cylindrical shape and dimension were selected to ensure experimental consistency. The average roundness, sphericity, and cylindricity were 0.161, 0.026, and 0.705, respectively. Drying experiments aimed to achieve a final moisture content below 13.5% on a wet basis, in accordance with the Thai Agricultural Standard for dried chili peppers (TAS 3001-2010) [28].

2.2 Experimental Setup

The drying tests were carried out using a hot-air convective dryer (HACD) in the Department of Mechanical and Mechatronics Engineering, Prince of Songkla University, Thailand. The structure of the HACD is illustrated in Figure 4. In this case, the HACD was working as a forced convection thermo-fluid dryer that used heated air flow to provide thermal energy to the chilies' surface and, at the same time, extract the moisture from the drying chamber via heat and mass transfer processes. The HACD was comprised of a stainless-steel drying chamber (1500 × 600 × 1000 mm^3) with five perforated trays (3 mm thickness), a 500 mm heating chamber with four 4000W heaters, 200 mm inlet and outlet pipes with perforated plates to achieve homogeneous air distribution, and 50 mm insulation material to minimize heat losses.

In this context, the phrase "direct-heating air tray" means that the heated forced airflow comes into contact with the perforated trays holding the product layers in the drying chamber. This method of air drying differs from conventional tray drying methods in which the airflow does not easily penetrate into the product layers. This allowed for more efficient air flow passage and direct heating of the TJCP surface. The design of the perforated trays enabled the hot air to flow uniformly throughout the layers of the product, which ensured that no areas of stagnant air existed within the chamber and uniform temperatures were attained. The electrical heaters provided the necessary thermal energy that was used to increase the air temperature, thus improving the temperature difference between the air and the surface of the chilies. This led to increased convection and heat transfer, as well as evaporation of moisture from the chilies. The placement of the perforated plates at the entry and exit points ensured better flow of the air into and out of the chamber. Thermal insulation minimized the conduction losses in the process of heat removal.

Airflow was generated by a three-phase blower governed via a digital inverter and quantified using a digital anemometer. The blower produced forced airflow through the drying chamber, increasing airflow momentum and turbulence intensity, which enhanced convective heat and mass transfer between the drying air and TJCP surfaces. Higher airflow velocity also reduced the thermal and concentration boundary layer thicknesses surrounding the chili surface, thereby accelerating moisture transport during drying. The system temperature was monitored using T-type

thermocouples and regulated by a temperature controller connected to a digital data logger (Graphtec GL240) with a measurement sensitivity of ±0.1 °C.

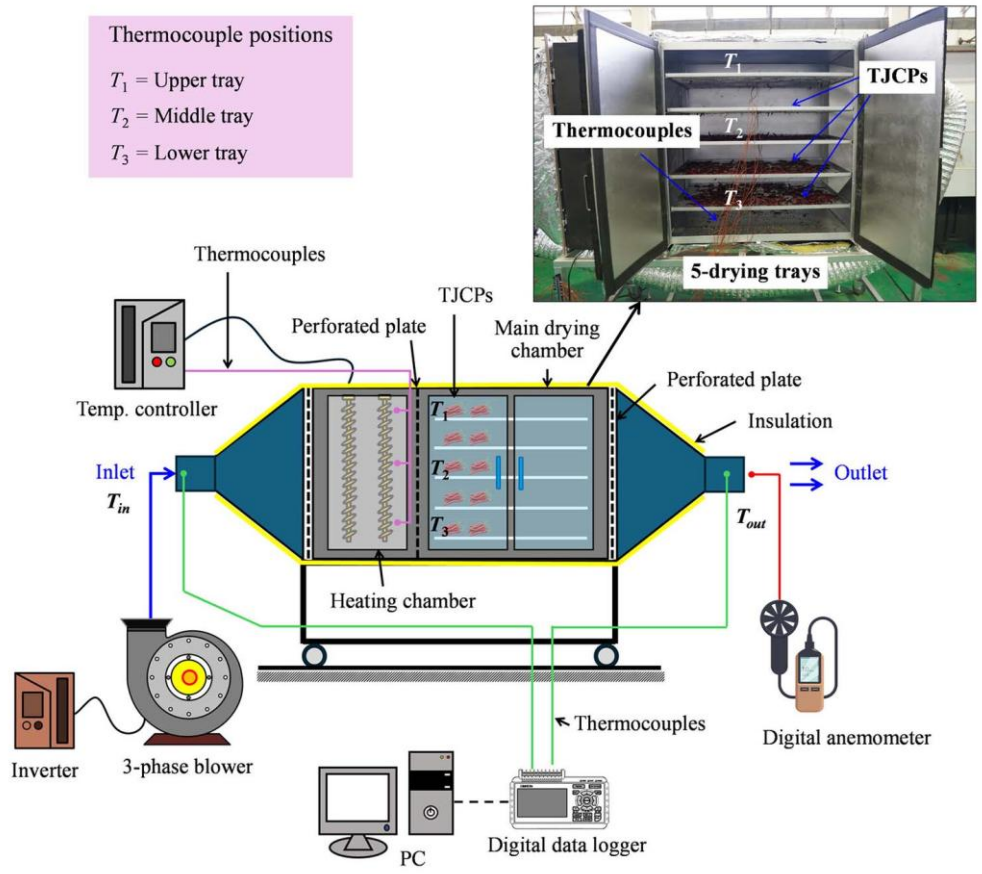

Figure 4. Schematic diagram of the direct-heating hot-air convective drying system showing heater location, airflow direction, thermocouple positions, and anemometer measurement point

Before carrying out the tests, the thermocouples and anemometer were calibrated by means of standard laboratory devices to ensure that reliable readings would be obtained. The T-type thermocouples were calibrated using a standard temperature calibration bath, while the digital anemometer was calibrated by use of a standard flow measuring device before conducting the experiment. The uncertainty of measurements was kept to an acceptable laboratory level. Thermocouples were positioned at different vertical and streamwise locations within the drying chamber to monitor the temperature distribution and evaluate thermal uniformity during the drying operation. The sensor arrangement was selected to capture representative temperature variations across the airflow pathway and tray regions. Airflow velocity measurements were performed at the inlet section of the chamber, and the measurement location of the anemometer is indicated in Figure 4.

The temperature during the drying process was maintained at 55 °C, 60 °C, 65 °C, 70 °C, and 75 °C, while the Reynolds number (*Re*) was maintained at 20000, 30000, 40000, and 50000 (Table 1). The choice of this particular Reynolds number range reflected the forced convection airflow process within the drying chamber that could be employed for investigating the effect of flow hydrodynamics on drying process, heat transfer improvement, and moisture elimination process. The Reynolds number was adopted to describe the airflow process and convective mass transport behavior within the drying chamber. Higher Reynolds numbers indicated greater turbulence of the air stream flow, which in turn reduced the thickness of both thermal and concentration boundary layers on the TJCP. Under forced convection conditions, the heat transfer characteristics can be described using dimensionless relationships involving Reynolds number (*Re*), Nusselt number (*Nu*), and Prandtl number (*Pr*), as expressed by:

$$Nu = CNu^m Pr^n \tag{4}$$

where *C*, *m*, and *n* are empirical constants depending on the flow configuration and thermal boundary conditions. Since the convective heat transfer coefficient (*h*) is directly related to the Nusselt number, increasing the Reynolds number generally improves convective heat transfer performance and moisture evaporation efficiency inside the drying chamber.

The airflow velocity was measured at the outlet section of the drying chamber using a digital anemometer and was subsequently used to calculate the Reynolds number (*Re*) based on:

$$Re = \frac{\bar{V} D_h}{\nu} \tag{5}$$

where $\bar{V}$ is the mean air velocity, D_h is the hydraulic diameter, and v is the air's kinematic viscosity.

Table 1. Details of the experimental parameters

Parameters	Values
Drying temperature, T (°C)	55, 60, 65, 70, and 75
Reynolds number, Re	20000, 30000, 40000, and 50000

The TJCP samples were weighed every 30 minutes through an electronic balance (PR4202 OHAUS, ±0.01 g accuracy), which was done within 15 seconds to avoid any losses due to temperature decrease. Drying continued until the final moisture content fell below 10% (wet basis). All experiments were conducted in triplicate under identical operating conditions to ensure repeatability and consistency of the experimental results.

2.3 Data Reduction

The moisture content (*MC*) was determined using the AOAC method [29] in triplicate, and the results were averaged. *MC* was calculated as follows:

Wet basis:

$$MC_{wb}(\%) = \frac{W_i - W_f}{W_i} \times 100 \tag{6}$$

Dry basis:

$$MC_{db}(\%) = \frac{W_i - W_f}{W_f} \times 100 \tag{7}$$

where W_i and W_f are the initial and final weights, respectively.

The moisture ratio (*MR*) was calculated by:

$$MR = \frac{M_t - M_e}{M_i - M_e} \tag{8}$$

where M_t, M_i, and M_e are the moisture contents at time *t*, initial, and equilibrium, respectively. In the present study, the equilibrium moisture content (M_e) was assumed to be negligible because its value was considerably smaller than the instantaneous moisture content during most stages of hot-air drying. Under the investigated drying temperatures and airflow conditions, the relative humidity inside the drying chamber remained sufficiently low, resulting in minimal influence of M_e on the moisture ratio calculation. This simplification is commonly adopted in thin-layer drying analyses reported in previous drying studies. Since M_e is negligible compared to M_i, the equation simplifies to:

$$MR = \frac{M_t}{M_i} \tag{9}$$

The drying rate (*DR*) was calculated by:

$$DR = \frac{M_{t+\Delta t} - M_t}{\Delta t} \tag{10}$$

where $M_{(t+\Delta t)}$ is the moisture content at $t+\Delta t$, and t is the drying time.

Effective moisture diffusivity (D_{eff}) was estimated assuming the sample as an infinite slab [30], using Fick's second law:

$$MR = \frac{8}{\pi^2} exp\left(-\frac{\pi^2 t D_{eff}}{H^2}\right) \tag{11}$$

where H is half the thickness of the TJCP flesh (6.1 × 10-3 m). D_{eff} was determined from the slope (B) of the linear plot of ln (*MR*) versus drying time:

$$D_{eff} = -\frac{BH^2}{\pi^2} \tag{12}$$

Meanwhile, the activation energy (E_a) was calculated using the Arrhenius relationship [31, 32]:

$$D_{eff} = D_0 e^{\left[-\frac{E_a}{R(T+273.15)}\right]} \tag{13}$$

Taking the natural logarithm gives:

$$\ln D_{eff} = \ln D_0 - \frac{E_a}{R(T + 273.15)} \tag{14}$$

where D_0 is the diffusion coefficient at 273.15 K, and R is the universal gas constant (8.314 J/mol·K).

Statistical analysis was performed using analysis of variance (ANOVA) to evaluate the significance of drying temperature and Reynolds number on drying time and effective moisture diffusivity. Experimental data are presented as mean ± standard deviation based on triplicate measurements. Differences were considered statistically significant at $p < 0.05$.

2.4 Uncertainty Analysis

The experimental measurement uncertainties were estimated using Moffat's method [33]. The combined uncertainty (δR) of dependent parameters was calculated by:

$$\delta R = \sqrt{\left\{\sum_{i=1}^{N}\left(\frac{\partial R}{\partial X_i}\delta X_i\right)^2\right\}} \tag{15}$$

where X_i represents independent variables, and δX_i their associated uncertainties. Tables 2 and 3 summarize the uncertainties of all measured and derived quantities.

Table 2. The uncertainty values for the measured parameters

Parameters	Symbol	Instrument	Uncertainties
Shape of the TJCPs	*D*, *L*	Digital vernier caliper	±0.01 mm
Velocity	$\bar{V}$	Digital anemometer	±0.1 m/s
Temperature	*T*	Digital data logger (Graphtec GL240)	±0.1 °C
Weight of the TJCPs	*W*	Electronic balance (PR4202 OHAUS)	±0.01 g

Table 3. The experimental uncertainty

Results	Symbols	Values	Range of uncertainty (%)
Moisture content	*MC*	6.769-300.583	1.01-1.48
Drying rate	*DR*	7.437($\times 10^{-4}$)-0.048	1.28-1.83
Reynolds number	*Re*	20000-50000	3.13-3.76
Effective moisture diffusivity	D_{eff}	0.374-5.176 ($\times 10^{-10}$)	0.47-1.02
Activation energy	E_a	40.028-102.333	0.021-0.27

3. Results and Discussion

3.1 Drying Time

Figure 5 compares the moisture ratio (*MR*) and drying time of TJCPs with previous drying techniques. Natural sun drying, as reported by Bhardwaj et al. [34], required over 75 hours due to fluctuating solar intensity and low heat transfer. The use of phase change materials (PCM) reduced drying time by 15-20 hours [35]. Hot-air drying further shortened the process to 8-10 hours [36], while jet drying methods decreased it to 6-8 hours [23].

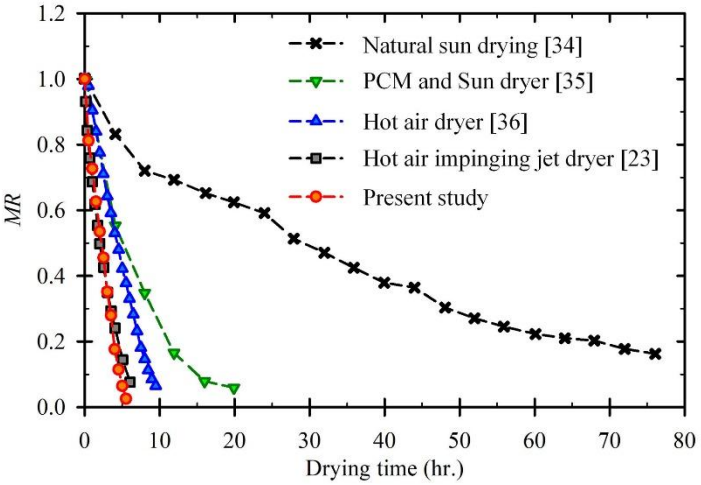

Figure 5. Moisture content and drying time of the TJCPs compared with previous drying techniques [23, 34-36]

In this current experiment, the direct-heating air tray method had the fastest drying rate of about 6-7 hours, attributed to improved thermo-fluid characteristics. The perforated tray design provided for more efficient airflow distribution and less stagnation of airflow within the chamber. On the other hand, the direct-heating method maintained a constant temperature throughout the drying process. Additionally, the induced convection airflow under high Reynolds number provided increased turbulence strength, leading to thinner boundary layers around the TJCP surface, thus increasing

convective heat and mass transfer coefficients. The above effects contributed to rapid evaporation of moisture, better temperature distribution between the trays, and a reduction in the resistance to moisture transfer.

3.2 Moisture Content and Moisture Ratio Behavior

3.2.1 Moisture content (dry basis)

Figure 6 shows the effect of temperature on moisture content (dry basis) with respect to drying time for different values of the Reynolds number (*Re*). There was a considerable increase in the rate of removal of moisture when the temperature of drying increased from 55 °C to 75 °C. This was true regardless of the level of *Re*, since an increase in temperature would increase the temperature gradient and vapor pressure difference between the surface of the TJCP and the air flow surrounding it. An increase in airflow or high *Re* would improve heat and mass transfer through convection, especially in the initial drying period.

The moisture reduction occurred at a faster pace during the first two hours, during which the rate of evaporation was constant since the surface moisture was easily evaporated owing to adequate heat energy supply as well as strong convective air flow. As drying continued beyond this phase, the rate of moisture evaporation slowed down because the remaining moisture had become entrapped inside the chili's internal structure. Consequently, moisture transport was controlled mainly by internal diffusion mechanisms rather than by external convective conditions, leading to a slower-falling-rate drying period.

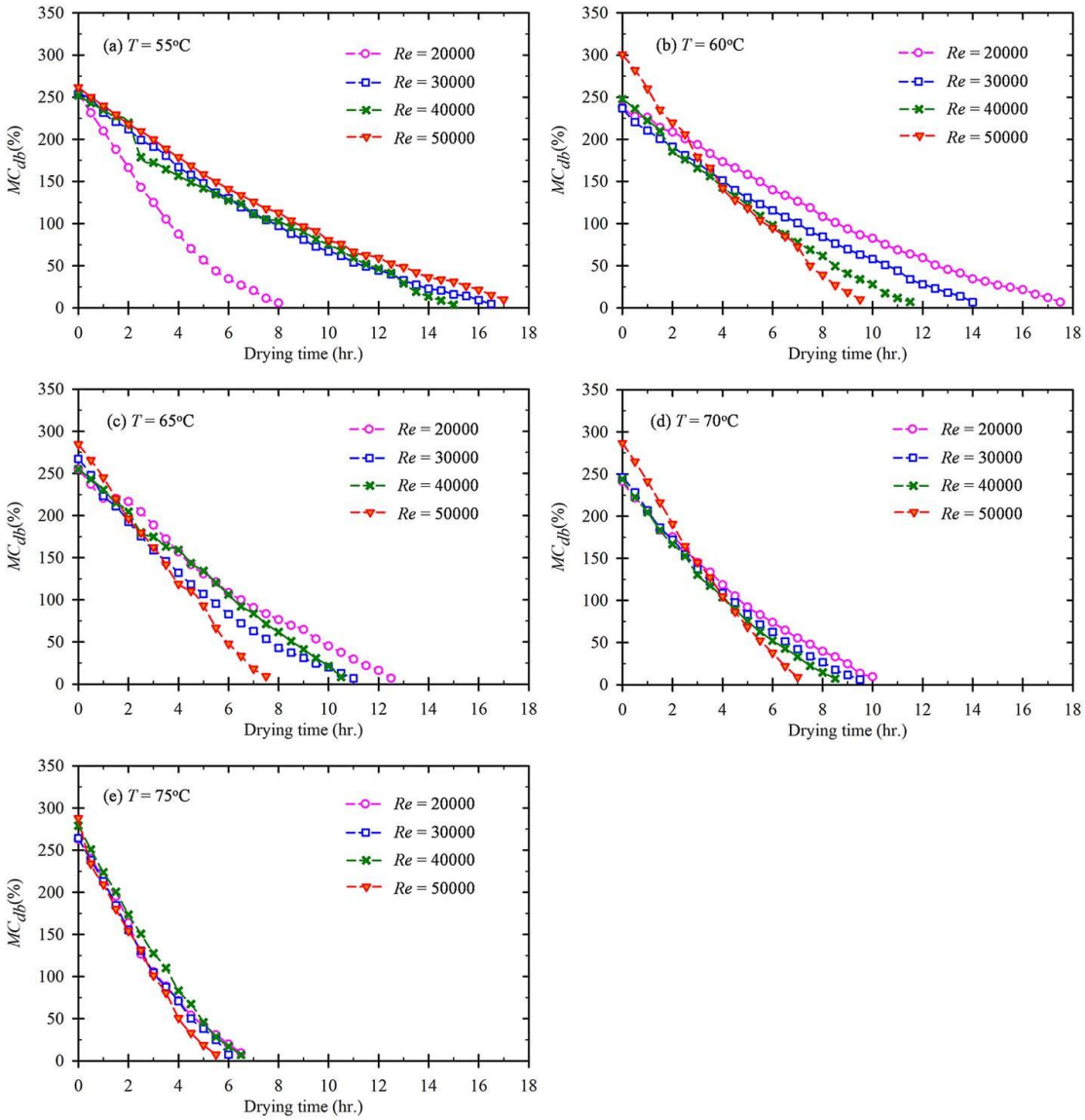

Figure 6. Comparison of moisture content (dry basis) with drying time for the TJCPs at different temperatures and Reynolds numbers

3.2.2 Moisture content (wet basis)

Profiles of moisture content on a wet basis are illustrated in Figure 7. Similarly, as in the case of moisture content analysis on a dry basis, high temperatures resulted in faster dehydration rates since high air temperatures provided higher heat energy to the products and increased the pressure gradient difference between the surfaces of the product and air flow,

hence increasing the evaporation of moisture content. At 75 °C, drying time was substantially shorter than at 55 °C, reflecting stronger convective heat transfer and accelerated moisture diffusion within the chili tissue

As the Reynolds number (*Re*) was increased, the rate of drying became more efficient due to an increase in the momentum of airflow, turbulence intensity, and convection within the dryer chamber. The circulation of air resulted in thinner thermal and concentration boundary layers around the chilies' surface, promoting moisture transfer into the airflow. There were two different drying stages, which included an initial rapid drying stage and a slower diffusion-controlled stage. In the first drying stage, the free water present at the surface dried out quickly since convective transfer processes played a dominant role during drying. As drying proceeded further, the remaining water got more tightly bound with the inner cellular structures of the TJCPs, which resulted in the drying being controlled by internal diffusion resistance. Hence, the drying rate slowed down in the latter drying stage.

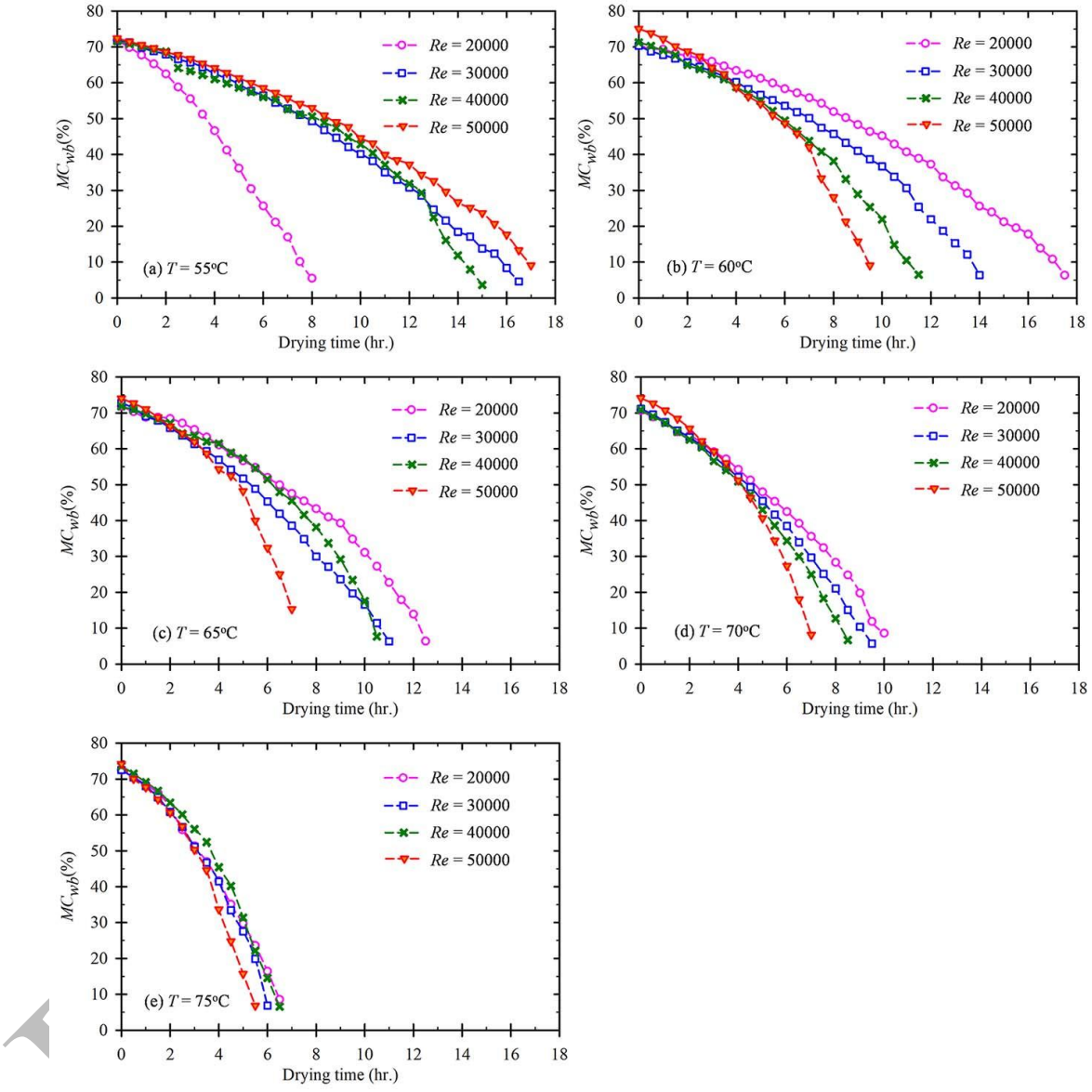

Figure 7. Comparison of moisture content (wet basis) with drying time for the TJCPs at different temperatures and Reynolds numbers

3.2.3 Moisture ratio

In Figure 8, the moisture ratio (*MR*) against the drying time is presented. As observed in the plot, an increase in temperature reduced *MR* more quickly. This confirmed that temperature plays a predominant role in the drying process. Although the increase in *Re* improves drying time, this improvement became more obvious at lower temperatures. In addition, an increase in the Reynolds number resulted in forced convection and thus reduced the thickness of both the hydrodynamic and thermal boundary layer. This led to a higher convective heat transfer coefficient, which increased moisture transport from the surface of the product into the drying air flow, especially during the first stage of the drying operation when the moisture was on the surface of the product. This improvement in convective heat transfer coefficient is as expected since the increase in Reynolds number usually enhances the Nusselt number and hence the convective heat

transfer coefficient in line with *Re-Nu-Pr* relations. In such cases, strong air flow led to effective heat transfer from the hot air to the TJCP surface.

With increased temperatures, the thermal gradient played a much larger role than the effect of airflow velocity. Additionally, increased air movement circulation because of a higher Reynolds number resulted in better distribution of air and temperature within the drying chamber and less moisture accumulation in the system, hence leading to more uniform drying behavior. This study shows that both thermal energy input and air dynamics play an integral part in controlling the heat and mass transfer phenomena during hot air convection drying.

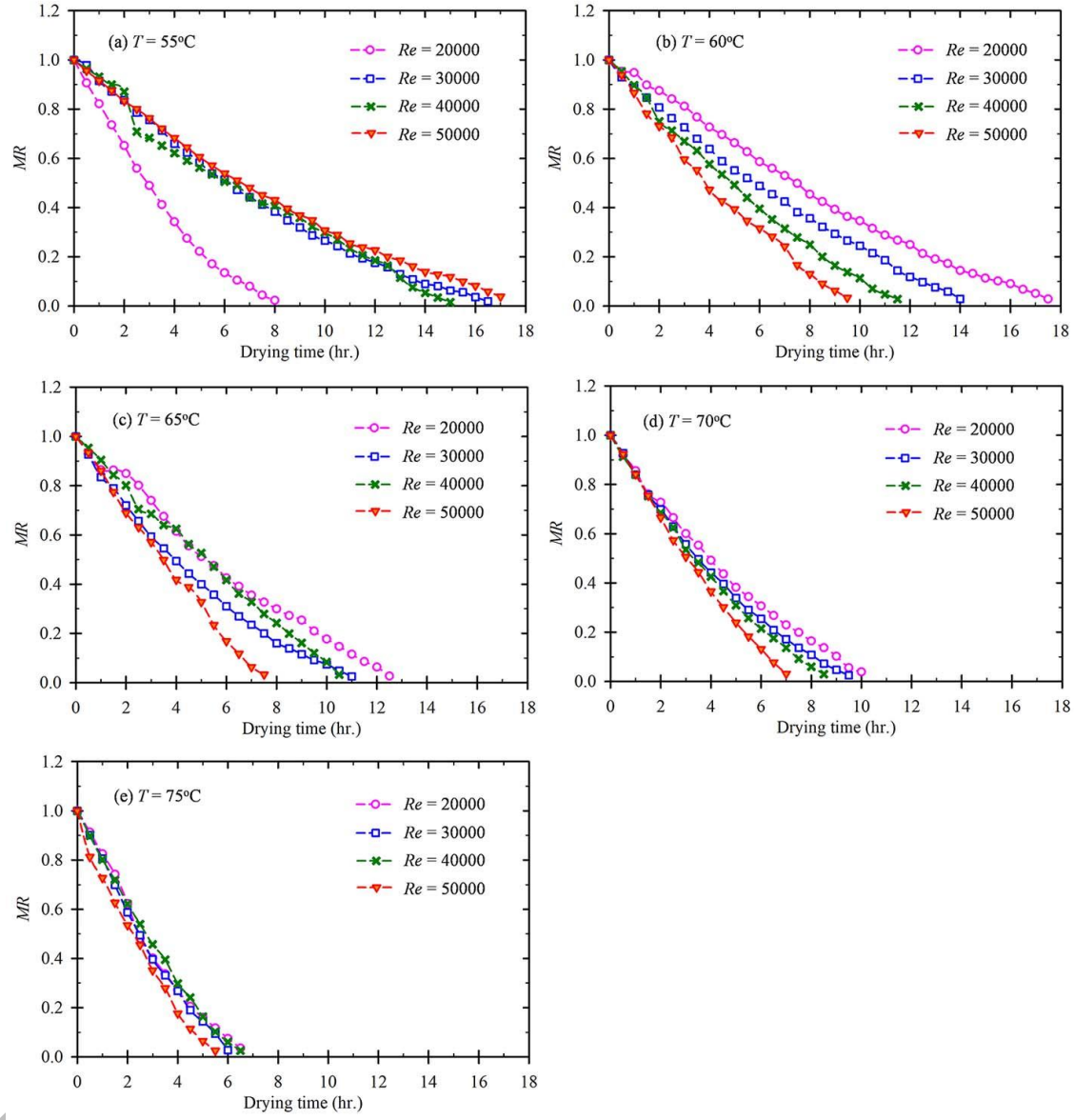

Figure 8. Comparison of moisture ratio with drying time for the TJCPs at different temperatures and Reynolds numbers

3.2.4 Drying rate analysis

Drying rate with respect to drying time has been plotted in Figure 9. Initially, the rate of drying was relatively high since water evaporation from the surface was predominant, but later on, it fell drastically because internal diffusion took over. The drying temperature raised the difference in vapor pressure between the surface of the TJCP and the surrounding air flow, thus increasing convective mass transfer and promoting faster evaporation during the constant-rate period. Just like increased *Re*, an enhanced rate of drying was recorded during the initial phase because of enhanced convection heat transfer. High *Re* values meant high forced air flow and turbulence in the enclosure, leading to low thermal resistance at the surface of the sample and better penetration of heat in the structure of TJCP. Enhanced airflow further ensured that moisture vapor was carried away faster from the surface of the sample.

In relation to thermo-fluid dynamics, increasing the Reynolds number led to higher flow momentum and turbulence inside the drying chambers, leading to better convective transport effectiveness and heat transfer coefficients. This led to better temperature distribution amongst the trays due to better air flow circulation inside the chamber. Increased drying efficiency at high Reynolds numbers was a result of improved convection processes, whereby improved airflow

circulation resulted in increased values of the Nusselt number and convective heat transfer coefficients, thus speeding up evaporation.

The Reynolds number value of *Re* = 50000 always led to the fastest drying process. For this value, the forced convection was high enough that it contributed significantly to improving the heat transfer and the mass transfer, making it the most efficient condition for the drying process among all conditions tested. In terms of energy transfer, the decreased drying time at high Reynolds numbers and temperatures implies that there is better utilization of the thermal energy supplied to evaporate the moisture. The increase in flow of air resulted in better distribution of thermal energy within the chamber as well as reduced localization of moisture. As drying progressed, the drying rate gradually decreased because internal moisture diffusion became the controlling mechanism. During this falling-rate period, moisture migration from the inner structure of the chili to the surface became increasingly limited by internal resistance rather than external convective conditions.

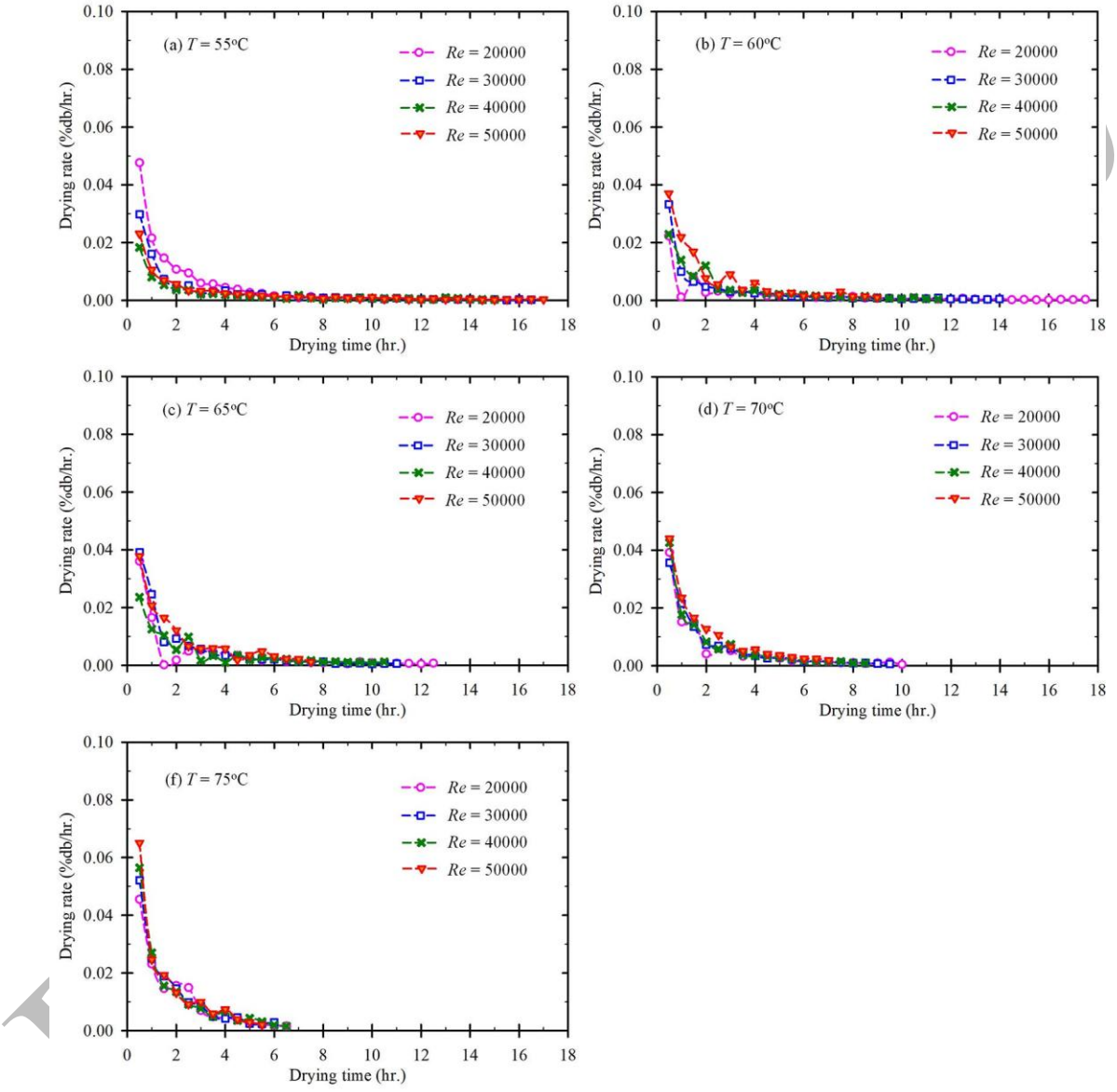

Figure 9. Comparison of drying rate with drying time for the TJCPs at different temperatures and Reynolds numbers

3.2.5 Effective moisture diffusivity and activation energy

The average value of effective moisture diffusivity (D_{eff}) and activation energy (E_a) determined through three sets of experiments in varying Reynolds numbers and drying temperatures is summarized in Table 4. It was observed that D_{eff} values were higher at high temperatures for all Reynolds numbers because of the high molecular mobility of water molecules. D_{eff} values were found to be higher at high Reynolds numbers at a particular temperature, which was due to high mass transfer because of higher flow of air. Higher D_{eff} values at high Reynolds numbers were because of better convective heat and mass transfer due to forced airflow system. Better turbulence and air circulation resulted in better heat transfer into the TJCP matrix, leading to better moisture diffusion.

As E_a decreased, the value of *Re* increased. This implies that the greater the airflow, the lower the energy barrier for moisture diffusion because more moisture may be removed from the surface, and turbulent action is induced. From a

thermodynamic point of view, higher airflow conditions helped transport thermal energy to the surface of the product, resulting in reduced external mass transfer resistance, facilitating internal moisture diffusion. Less activation energy was therefore required to initiate moisture diffusion under high-*Re* conditions.

Table 4. Effective moisture diffusion coefficients and activation energies of TJCPs under different *Re* and *T*

Re	*T* (°C)	D_{eff} ($\times 10^{-10}$ m^2/s)	E_a (kJ/mol)
20000	55	0.374	102.333
	60	1.437	
	65	1.958	
	70	2.524	
	75	4.118	
30000	55	1.714	44.880
	60	1.771	
	65	2.564	
	70	2.966	
	75	4.331	
40000	55	1.727	40.028
	60	2.247	
	65	2.123	
	70	3.125	
	75	4.216	
50000	55	1.450	54.298
	60	2.642	
	65	3.295	
	70	3.586	
	75	5.176	

The maximum activation energy of 102.33 kJ/mol was recorded at Reynolds number 20000; this means that the moisture diffusion was most resistant at this point. Conversely, the minimum activation energy of 40.03 kJ/mol was registered at Reynolds number 40000. The substantial drop in the value of activation energy from *Re* = 20000 to *Re* = 30000 is due to the shift from the relatively weak forced convection to more intensified hydrodynamic air flow within the drying chamber. Thickening of thermal and concentration boundary layer at *Re* = 20000 could have led to increased external resistance for both heat and mass transport, and hence higher activation energy for moisture diffusion. With the increase in the Reynolds number to 30000 and 40000, the convective heat transfer improved due to stronger air flow circulation and turbulence intensities. This made surface drying more efficient because of low mass transfer resistance from outside. This meant that there was an improvement in the transport of thermal energy from air to the surface of chilies, thus making it easier for internal moisture movement with less energy use. From the thermodynamic point of view, forced convection efficiency improves heat energy usage efficiency, hence reducing activation energy significantly. The significant drop in activation energy from Re=20000 to Re=40000 clearly signifies the impact of the hydrodynamics of the airflow on coupled heat and mass transfer process. An increase in Reynolds number implies increased efficiency in the transfer of thermal energy due to better forced convection, which in turn results in lower resistance to the diffusion of moisture within.

Indeed, the results of ANOVA indicated that both drying temperature and Reynolds number have a significant influence on the drying time and effective moisture diffusivity at the level of $p < 0.05$. Higher values of temperature and Reynolds numbers were significantly favorable for drying efficiency and moisture transport characteristics. Table 5 shows comparisons between the current findings and the existing literature. Previous research on red chili peppers gave values for effective moisture diffusivity ranging from 1.33 to 71 × 10^{-10} m²/s, while the values of activation energy ranged from 23.35 kJ/mol to 50.9 kJ/mol [23, 36, 37]. The values of effective moisture diffusivity found in the TJCPs in the current study were comparatively less than those in the previous literature and ranged from 0.374 to 5.176 × 10^{-10} m²/s, indicating comparatively slower movement of water molecules within TJCPs during drying. In terms of activation energy, its value ranged from 40.03 to 102.33 kJ/mol, which implies that the energy of moisture diffusion was greatly affected by the drying air flow and temperature.

Relatively low values of D_{eff} for the TJCP samples in comparison to other types of red chilies are due to differences in structural properties inherent in the specific cultivar. The chili peppers of the Thai Jinda variety have relatively compact internal tissues and a thick outer skin layer that could increase their internal resistance to the migration of moisture during the drying process. Besides, the natural waxy coating of the fruit surface may restrict moisture diffusion and reduce evaporation rates. The particular design of the dryer might also be responsible for the observed diffusivity properties. While the use of the direct-heating perforated tray setup helped achieve better distribution of the airflow and increased convection, the way that airflow penetrates the dense chili layer might hinder internal mass transfer more than is the case for thinner slices of other plants. This trend is in line with earlier studies conducted on drying of chili pepper and other

agricultural products using hot air dryer, which showed that an increase in flow rate and drying temperature increased moisture diffusion and decreased drying resistance by improved convective heat and mass transfer [23, 36, 37].

Table 5. The activation energies and effective moisture diffusivity values of chili peppers and some other agricultural items

Authors	Products	T (°C)	D_{eff} ($\times 10^{-10}$ m^2/s)	E_a (kJ/mol)
Zheng et al. [23]	Red chili pepper	50-80	1.33-8.97	46.59-50.9
Scala and Crapiste [36]	Red chili pepper	20-50	5.01-8.32	23.35
Kaleemullah and Kailappan [37]	Red chili pepper	50-65	37.8-71	37.76
Ju et al. [38]	Yam slice	50-70	5.55-10.8	29.53
Xie et al. [31]	Wolfberry	60-70	3.72-7.31	54.3
Xiao et al. [39]	Monukka seedless grapes	50-65	1.82-5.85	67.29
Dai et al. [40]	Apricot	50-70	2.19-11.02	31.4-74.18
Present study	TJCPs	55-75	0.374-5.176	40.028-102.333

3.2.6 Visual appearance of dried products

Figure 10 shows a comparison between the samples of TJCPs dried in the present study (T = 60 °C, Re = 40000) and those available in the market. Samples dried in this study were more vibrant red in color, evenly dried, and had a smooth surface, while the samples from the market were dull in color and had uneven surfaces because of improper drying. This shows that the current method of HACD preserves color and attractiveness, which are important aspects in making a product attractive and marketable.

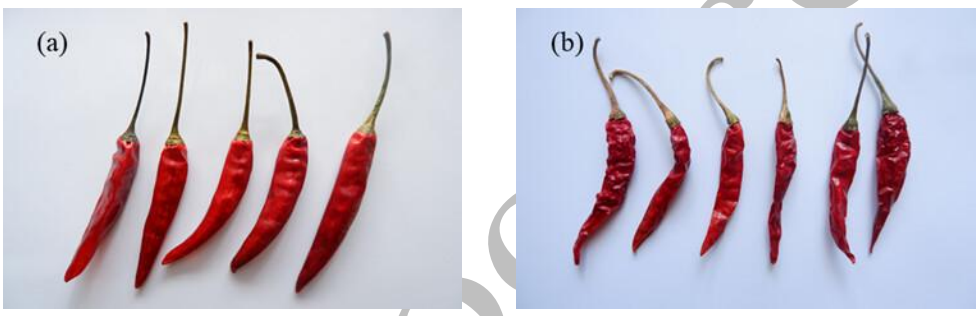

Figure 10. Comparison of TJCP dried products from (a) the present study (T = 60 °C, Re = 40000) and (b) the local market

4. Conclusions

In this experimental study, the influence of drying temperatures and air flows (Reynolds numbers) on the drying characteristics and quality properties of Thai Jinda chili peppers (TJCPs) has been investigated by employing a direct-heating air tray system. The drying process is treated as a combined thermo-fluid problem considering forced convective heating and intragranular moisture diffusion. The main findings are as follows:

- The effectiveness of drying greatly increased with an increase in drying temperature from 55 °C to 75 °C and an increase in Reynolds number from 20000 to 50000. In low temperatures, air velocity was very effective, while in high temperatures, temperature was the most influential variable in removing moisture. The increase in the Reynolds number improved the forced convection within the drying chamber and therefore improved the performance of air flow and convective heat transfer in the process. The high Reynolds number caused an increase in turbulence level and also decreased the thermal and concentration boundary layer thickness around the TJCP.
- The drying rate trends indicated that the rapid drying process occurred in the early drying phase when the temperature was high and Re = 50000. Such conditions resulted in minimum drying times and maximum heat and mass transfers. The better drying performance achieved at high Reynolds numbers was due to the thinness of both thermal and concentration boundary layers around the chili. As a result, moisture could evaporate faster, and the resistance to external mass transfer became smaller. An increase in forced convection would result in better air flow distribution and uniform temperatures within the chamber, hence resulting in better drying of the trays. Further, better airflow circulation also ensured higher efficiency of thermal energy transfer from the hot air to the TJCP sample surface and hence faster evaporation.
- The effective moisture diffusivity was observed to increase with increasing temperature and air velocity, whereas activation energy decreased with an increase in the Reynolds number, thus suggesting improved internal moisture transfer with increasing forced convection effects. In comparison to other agricultural samples previously analyzed, the TJCPs showed moisture diffusion rates that were comparatively lower, but they had a broad range of activation energy values from 40.03 to 102.33 kJ/mol, indicating the moisture diffusion behavior of this particular cultivar to be highly responsive to the temperature and flow conditions.
- Using the direct-heating air tray system resulted in the least amount of time for drying, at around 6–7 hours, compared to other drying systems. It was less time-consuming than the natural sun drying system, which takes about 75 hours

to dry, the PCM-assisted drying system, which needs 55–60 hours to dry, and the hot-air drying system, which took about 8-10 hours. The perforated trays were efficient in attaining a uniform temperature distribution within the drying chambers.

- The quality of the products was high, with the dried TJCPs having vibrant red color, smooth skin, and uniform appearance compared to their counterparts from the local market, showing the efficiency of the controlled drying process.

In contrast with most of the previous drying studies, which have only been concerned with empirical drying data, the current study has focused on the thermos-fluid aspects of the drying process through examining the impact of Reynolds number-dependent airflow on convective heat transfer, moisture transport, activation energy, and uniformity of drying using the direct-heating perforated tray drying system. The behavior of drying matched theoretical models related to forced convection heat transfer, where higher values of Reynolds number increased air flow mixing and thus convective heat transfer efficiency, thereby improving the drying process. This indicates that air flow hydrodynamics have an important effect on heat and mass transfer in the drying chamber.

Even without the determination of energy-efficiency values such as Specific Energy Consumption (SEC), Specific Moisture Extraction Rate (SMER), and thermal efficiency, the results have clearly shown that enhanced forced convection led to better thermal energy utilization and drying efficiency. Future studies on this topic need to focus on incorporating real-time energy consumption for proper thermo-economic evaluation of the system. In terms of mechanical engineering considerations, the direct-heated air tray dryer was capable of providing good airflow distribution and convective transport for faster drying and more uniform products. The optimized convective drying of chilies through direct-heated air trays is thus a practical way to dry chilies in the industry by minimizing drying time and increasing product quality.

Acknowledgements
The authors would like to thank the Department of Mechanical and Mechatronics Engineering, Prince of Songkla University, for providing the facilities and workspace necessary to conduct the experiments.

Funding
This work was supported by the National Science, Research and Innovation Fund (NSRF) and Prince of Songkla University under Grant No. ENG6701083S.

Declaration of Competing Interest
The authors declare no conflicts of interest.

CRediT Authorship Contribution Statement
Ni-Asri Cheputeh: Writing – original draft, Review and Editing
Natthaporn Kaewchoothong: Formal analysis, Project administration, Funding acquisition, Investigation, Methodology, Resources, Visualization, Writing – Original Draft, Review and Editing

Availability of Data and Materials
The data supporting this study's findings are available on request from the corresponding author.

Ethics Statement
This study did not involve human participants or animal subjects. Ethical approval was therefore not required for this research.

Generative Artificial Intelligence Declarations
The authors claim that artificially intelligent-assisted technologies, such as generative AI, were not used to generate content, ideas, or theories. We have just utilized AI to enhance readability and refine the language. This was used with extreme human control and oversight. The authors take full responsibility for reviewing and approving the content.

References
[1] E. J. Rifna, M. Dwivedi, O. Chauhan, "Role of water activity in food preservation," in *Advances in Food Chemistry*, 2022, pp. 39–64. https://doi.org/10.1007/978-981-19-4796-4_2
[2] O. Benedicta Adewoyin, "Pre-harvest and postharvest factors affecting quality and shelf life of harvested produce," in *New Advances in Postharvest Technology*, İ. Kahramanoğlu Ed. London: IntechOpen, 2023. https://doi.org/10.5772/intechopen.111649
[3] S. Tepthanee, J. Taweekun, P. Vessakosol, "Application of passive technique to cocoa beans batch dryer and assessment of thin layer models," *International Journal of Automotive and Mechanical Engineering*, vol. 21, no. 2, pp. 11398–11414, 2024. https://doi.org/10.15282/ijame.21.2.2024.17.0880
[4] M. S. Rana, A. N. M. A. Rahman, R. Ahmed, et al., "Design, fabrication, and performance evaluation of a food solar dryer," *AgriEngineering*, vol. 6, no. 4, pp. 4506–4523, 2024. https://doi.org/10.3390/agriengineering6040257
[5] M. K. Rizalman, E. G. Moung, J. A. Dargham, Z. Jamain, N. M. Yaakub, S. Omatu, "Internet-of-things for smart dryers: Enablers, state of the arts, challenges, and solutions," in *2022 IEEE International Conference on Artificial*

Intelligence in Engineering and Technology (IICAIET), 13–15 Sept 2022, pp. 1–6. https://doi.org/10.1109/IICAIET55139.2022.9936770

[6] A.-H. Mohammed, C. A. Komolafe, A. Simons, "Advances in solar drying technologies: A comprehensive review of designs, applications, and sustainability perspectives," *Solar Compass*, vol. 17, 2026. https://doi.org/10.1016/j.solcom.2025.100153

[7] V. Shrivastava, P. Singh, N. Shrivastava, "A decade of progress in indirect solar drying: A review of systems for fruits, vegetables, and medicinal herbs (2015–2025)," *Renewable and Sustainable Energy Reviews*, vol. 226, 2026. https://doi.org/10.1016/j.rser.2025.116388

[8] L. Rajapaksha, D. M. C. C. Gunathilake, S. M. Pathirana, T. N. Fernando, "Reducing post-harvest losses in fruits and vegetables for ensuring food security – Case of Sri Lanka," *MOJ Food Processing & Technology*, vol. 9, no. 1, pp. 7–16, 2021. https://doi.org/10.15406/mojfpt.2021.09.00255

[9] K. O. Obondo, L. M. Waswa, "The level of adoption of vegetable sun-drying technology in Teso South Sub County, Kenya," *Journal of the Kenya National Commission for UNESCO*, vol. 5, no. 2, 2025. https://doi.org/10.62049/jkncu.v5i2.317

[10] J. F. Hinojosa, S. F. Moreno, V. M. Maytorena, "Low-temperature applications of phase change materials for energy storage: A descriptive review," *Energies*, vol. 16, no. 7, 2023. https://doi.org/10.3390/en16073078

[11] D. P. García-Moreira, I. Moreno, E. C. López-Vidaña, "Controlled solar drying as a sustainable strategy to preserve color and minimize food waste," *AgriEngineering*, vol. 7, no. 11, 2025. https://doi.org/10.3390/agriengineering7110392

[12] S. A. Siddiqui, İ. l. Ucak, S. Jain, et al., "Impact of drying on techno-functional and nutritional properties of food proteins and carbohydrates - A comprehensive review," *Drying Technology*, vol. 42, no. 4, pp. 592–611, 2024. https://doi.org/10.1080/07373937.2024.2303580

[13] S. Lal, M. K. Mahatma, S. N. Saxena, et al., "Influence of drying methods on preservation of colour and quality attributes in celery (Apium graveolens L.) and dill (Anethum graveolens L.) leaves," *Applied Food Research*, vol. 6, no. 1, 2026. https://doi.org/10.1016/j.afres.2026.101694

[14] T. Saengsuwan, N. Sujinda, "Integrated performance assessment of vacuum heat pump drying: a multi-criteria framework for energy-quality optimization in banana slice drying," *Sustainable Food Technology*, vol. 4, no. 1, pp. 894–915, 2026. https://doi.org/10.1039/D5FB00546A

[15] O. Nnamchi, C. Tom, G. Akpan, et al., "Solar dryers: A review of mechanism, methods and critical analysis of transport models applicable in solar drying of product," *Green Energy and Resources*, vol. 3, no. 2, 2025. https://doi.org/10.1016/j.gerr.2025.100118

[16] H. M. Elmatsani, S. J. Munarso, B. Benyamin, et al., "Global perspective on red chili drying: insights from two decades of research (2004–2023)," *Frontiers in Sustainable Food Systems*, vol. 8, 2024. https://doi.org/10.3389/fsufs.2024.1456938

[17] E. S. P. Yap, A. Uthairatanakij, N. Laohakunjit, P. Jitareerat, "Influence of hot air drying on capsaicinoids, phenolics, flavonoids and antioxidant activities of 'Super Hot' chilies," *PeerJ*, vol. 10, p. e13423, 2022. https://doi.org/10.7717/peerj.13423

[18] A. Krzykowski, S. Rudy, R. Polak, et al., "Drying of Red Chili Pepper (Capsicum annuum L.): Process kinetics, color changes, carotenoid content and phenolic profile," *Molecules*, vol. 29, no. 21, Oct 31 2024. https://doi.org/10.3390/molecules29215164

[19] F. Ajuebor, O. A. Aworanti, O. O. Agbede, S. E. Agarry, T. J. Afolabi, O. O. Ogunleye, "Drying process optimization and modelling the drying kinetics and quality attributes of dried chili pepper (Capsicum frutescens L.)," *Trends in Sciences*, vol. 19, no. 17, 2022. https://doi.org/10.48048/tis.2022.5752

[20] J. O. Ojediran, C. E. Okonkwo, A. F. Olaniran, et al., "Hot air convective drying of hog plum fruit (Spondias mombin): effects of physical and edible-oil-aided chemical pretreatments on drying and quality characteristics," *Heliyon*, vol. 7, no. 11, p. e08312, Nov 2021. https://doi.org/10.1016/j.heliyon.2021.e08312

[21] L. A. Espinoza-Espinoza, C. E. Juárez-Ojeda, L. A. Ruiz-Flores, L. A. Moreno-Quispe, M. S. Anaya-Palacios, H. Cárdenas-Quintana, "Influence of convection drying with hot air on the physicochemical and phytochemical properties of green banana flour (Musa cavendish)," *Frontiers in Sustainable Food Systems*, vol. 7, 2023. https://doi.org/10.3389/fsufs.2023.1204349

[22] R. Bai, J. Sun, X. Qiao, Z. Zheng, M. Li, B. Zhang, "Hot air convective drying of ginger slices: drying behaviour, quality characteristics, optimisation of parameters, and volatile fingerprints analysis," *Foods*, vol. 12, no. 6, 2023. https://doi.org/10.3390/foods12061283

[23] Z. Zheng, S. Wang, C. Zhang, et al., "Hot air impingement drying enhanced drying characteristics and quality attributes of Ophiopogonis Radix," *Foods*, vol. 12, no. 7, 2023. https://doi.org/10.3390/foods12071441

[24] E. M. Goncalves, N. Pereira, M. Silva, et al., "Influence of air-drying conditions on quality, bioactive composition and sensorial attributes of sweet potato chips," *Foods*, vol. 12, no. 6, 2023. https://doi.org/10.3390/foods12061198

[25] S. Kaleemullah, R. Kailappan, "Geometric and morphometric properties of chillies," *International Journal of Food Properties*, vol. 6, no. 3, pp. 481–498, 2007. https://doi.org/10.1081/JFP-120021454

[26] Y. Keawsuntia, "Experimental investigation of active solar dryer for drying of chili," *Advanced Materials Research*, vol. 953-954, pp. 16–19, 2014. https://doi.org/10.4028/www.scientific.net/AMR.953-954.16

[27] M. Wae-hayee, K. Yeranee, W. Suksuwan, A. Alimalbari, S. Sae-ung, C. Nuntadusit, "Heat transfer enhancement in rotary drum dryer by incorporating jet impingement to accelerate drying rate," *Drying Technology*, vol. 39, no. 10, pp. 1314–1324, 2020.
[28] Ministry of Agriculture and Cooperatives, "Thai Agricultural Standard: Dried Chilli (TAS 3001-2010)," National Bureau of Agricultural Commodity and Food Standards, 2010 (in Thai). https://doi.org/10.1080/07373937.2020.1742150
[29] Association of Official Analytical Chemists Inc., "AOAC: Official Methods of Analysis (Volume 1)," 1990.
[30] İ. Doymaz, F. Kocayigit, "Effect of pre-treatments on drying, rehydration, and color characteristics of red pepper ('Charliston' variety)," *Food Science and Biotechnology*, vol. 21, no. 4, pp. 1013–1022, 2012. https://doi.org/10.1007/s10068-012-0132-z
[31] L. Xie, A. S. Mujumdar, X.-M. Fang, et al., "Far-infrared radiation heating assisted pulsed vacuum drying (FIR-PVD) of wolfberry (Lycium barbarum L.): Effects on drying kinetics and quality attributes," *Food and Bioproducts Processing*, vol. 102, pp. 320–331, 2017. https://doi.org/10.1016/j.fbp.2017.01.012
[32] M. Aghbashlo, M. H. kianmehr, H. Samimi-Akhijahani, "Influence of drying conditions on the effective moisture diffusivity, energy of activation and energy consumption during the thin-layer drying of berberis fruit (Berberidaceae)," *Energy Conversion and Management*, vol. 49, no. 10, pp. 2865–2871, 2008. https://doi.org/10.1016/j.enconman.2008.03.009
[33] R. J. Moffat, "Describing the uncertainties in experimental results," *Experimental Thermal and Fluid Science*, vol. 1, no. 1, pp. 3–17, 1988. https://doi.org/10.1016/0894-1777(88)90043-X
[34] A. K. Bhardwaj, R. Kumar, R. Chauhan, S. Kumar, "Experimental investigation and performance evaluation of a novel solar dryer integrated with a combination of SHS and PCM for drying chilli in the Himalayan region," *Thermal Science and Engineering Progress*, vol. 20, 2020. https://doi.org/10.1016/j.tsep.2020.100713
[35] L.-Z. Deng, X.-H. Yang, A. S. Mujumdar, et al., "Red pepper (Capsicum annuum L.) drying: Effects of different drying methods on drying kinetics, physicochemical properties, antioxidant capacity, and microstructure," *Drying Technology*, vol. 36, no. 8, pp. 893–907, 2017. https://doi.org/10.1080/07373937.2017.1361439
[36] K. Di Scala, G. Crapiste, "Drying kinetics and quality changes during drying of red pepper," *LWT - Food Science and Technology*, vol. 41, no. 5, pp. 789–795, 2008. https://doi.org/10.1016/j.lwt.2007.06.007
[37] S. Kaleemullah, R. Kailappan, "Modelling of thin-layer drying kinetics of red chillies," *Journal of Food Engineering*, vol. 76, no. 4, pp. 531–537, 2006. https://doi.org/10.1016/j.jfoodeng.2005.05.049
[38] H.-Y. Ju, C.-L. Law, X.-M. Fang, H.-W. Xiao, Y.-H. Liu, Z.-J. Gao, "Drying kinetics and evolution of the sample's core temperature and moisture distribution of yam slices (Dioscorea alataL.) during convective hot-air drying," *Drying Technology*, vol. 34, no. 11, pp. 1297–1306, 2015. https://doi.org/10.1080/07373937.2015.1105814
[39] H.-W. Xiao, C.-L. Pang, L.-H. Wang, J.-W. Bai, W.-X. Yang, Z.-J. Gao, "Drying kinetics and quality of Monukka seedless grapes dried in an air-impingement jet dryer," *Biosystems Engineering*, vol. 105, no. 2, pp. 233–240, 2010. https://doi.org/10.1016/j.biosystemseng.2009.11.001
[40] J.-W. Dai, J.-Q. Rao, D. Wang, et al., "Process-based drying temperature and humidity integration control enhances drying kinetics of apricot halves," *Drying Technology*, vol. 33, no. 3, pp. 365–376, 2015. https://doi.org/10.1080/07373937.2014.954667